Carbon residence time dominates uncertainty in terrestrial vegetation responses to future climate and atmospheric CO_2

Andrew D. Friend[a,1], Wolfgang Lucht[b,c], Tim T. Rademacher[a], Rozenn Keribin[a], Richard Betts[d], Patricia Cadule[e], Philippe Ciais[f], Douglas B. Clark[g], Rutger Dankers[d], Pete D. Falloon[d], Akihiko Ito[h], Ron Kahana[d], Axel Kleidon[i], Mark R. Lomas[j], Kazuya Nishina[h], Sebastian Ostberg[b], Ryan Pavlick[i], Philippe Peylin[f], Sibyll Schaphoff[b], Nicolas Vuichard[f], Lila Warszawski[b], Andy Wiltshire[d], and F. Ian Woodward[j]

[a]Department of Geography, University of Cambridge, Cambridge CB2 3EN, United Kingdom; [b]Potsdam Institute for Climate Impact Research, D-14412 Potsdam, Germany; [c]Department of Geography, Humboldt University, D-10099 Berlin, Germany; [d]Met Office Hadley Centre, Exeter EX1 3PB, United Kingdom; [e]Institute Pierre-Simon Laplace, 75252 Paris, France; [f]Laboratoire des Sciences du Climat et de l'Environnement, 91191 Gif-sur-Yvette, France; [g]Centre for Ecology and Hydrology, Wallingford OX10 8BB, United Kingdom; [h]Centre for Global Environmental Research, National Institute for Environmental Studies, Tsukuba, Ibaraki 305-8506, Japan; [i]Max Planck Institute for Biogeochemistry, D-07745 Jena, Germany; and [j]Department of Animal and Plant Sciences, University of Sheffield, Sheffield S10 2TN, United Kingdom

Edited by Katja Frieler, Potsdam Institute for Climate Impact Research, Potsdam, Germany, and accepted by the Editorial Board August 31, 2013 (received for review January 31, 2013)

Future climate change and increasing atmospheric CO_2 are expected to cause major changes in vegetation structure and function over large fractions of the global land surface. Seven global vegetation models are used to analyze possible responses to future climate simulated by a range of general circulation models run under all four representative concentration pathway scenarios of changing concentrations of greenhouse gases. All 110 simulations predict an increase in global vegetation carbon to 2100, but with substantial variation between vegetation models. For example, at 4 °C of global land surface warming (510–758 ppm of CO_2), vegetation carbon increases by 52–477 Pg C (224 Pg C mean), mainly due to CO_2 fertilization of photosynthesis. Simulations agree on large regional increases across much of the boreal forest, western Amazonia, central Africa, western China, and southeast Asia, with reductions across southwestern North America, central South America, southern Mediterranean areas, southwestern Africa, and southwestern Australia. Four vegetation models display discontinuities across 4 °C of warming, indicating global thresholds in the balance of positive and negative influences on productivity and biomass. In contrast to previous global vegetation model studies, we emphasize the importance of uncertainties in projected changes in carbon residence times. We find, when all seven models are considered for one representative concentration pathway × general circulation model combination, such uncertainties explain 30% more variation in modeled vegetation carbon change than responses of net primary productivity alone, increasing to 151% for non-HYBRID4 models. A change in research priorities away from production and toward structural dynamics and demographic processes is recommended.

DGVM | GVM | turnover | *NPP* | ISI-MIP

Terrestrial vegetation is central to many components of the coupled Earth system, in particular the global carbon cycle, biophysical land–atmosphere exchanges, atmospheric chemistry, and the diversity of life with the numerous ecosystem services this engenders. However, vegetation is very sensitive to climate and levels of atmospheric CO_2, the primary substrate for plant growth. Therefore, it is imperative that we are capable of anticipating the potential responses of global terrestrial vegetation to future changes in climate and atmospheric chemistry. However, a comprehensive, consistent analysis of impacts, taking into account uncertainty in both climate models and impacts models, has so far been lacking. The recent availability of representative concentration pathway (RCP)-driven climate model simulations, with bias-corrected outputs produced within the Inter-Sectoral Impact Model Intercomparison Project (ISI-MIP) (1), allows such an analysis.

Vegetation biomass, productivity, and the competitive abilities of different plant types are all influenced by climate and atmospheric CO_2. Higher temperatures will increase growing season lengths, metabolic rates, and rates of nitrogen mineralization at high latitudes and altitudes, thereby increasing productivity. However, they may reduce productivity in warmer areas through increased rates of evaporation and stomatal closure due to higher vapor pressure deficits. Increasing atmospheric CO_2 will tend to increase rates of photosynthesis and reduce evapotranspiration and/or increase leaf areas. It will also alter tissue stoichiometry, with significant repercussions for herbivores and soil decomposition. Furthermore, higher CO_2 will likely increase the competitive ability of plants that use the C_3 photosynthetic pathway relative to C_4 plants. Plant species have intrinsic ranges of potential water and nutrient use efficiencies, which will affect how they respond, and all plants will acclimate to changed forcings. Biomass is determined by inputs driven by photosynthesis and its allocation and outputs to senescence and mortality, each with their own environmental responses. However, global-scale vegetation model development has strongly focused on productivity processes whereas, apart from major disturbances such as fire, the dynamics of carbon turnover have been largely ignored.

Beginning in the 1990s, a handful of dynamic global vegetation models (DGVMs) have been developed, using parameterizations for many of the processes mentioned above. The first multi-DGVM study to look at the potential impacts of future climate and atmospheric CO_2 on global vegetation and soils was reported by ref. 2. This study looked at the responses of net ecosystem production (*NEP*), simulated by six DGVMs, to one climate and CO_2 change scenario, concluding that the major source of uncertainty in future *NEP* is the response of net primary productivity (*NPP*) to changing climate. Vegetation carbon (C_{veg}) was predicted to increase by an average of 270 Pg C from preindustrial levels across the models by 2100, but saturating *NPP* and increasing heterotrophic respiration led to a reduction in *NEP* after 2050.

Nine global vegetation models (GVMs) (meaning vegetation processes are simulated, but not necessarily vegetation dynamics),

Author contributions: A.D.F. and W.L. designed research; A.D.F., W.L., T.T.R., R. Keribin, R.B., P. Cadule, P. Ciais, D.B.C., R.D., P.D.F., A.I., R. Kahana, A.K., M.R.L., K.N., S.O., R.P., P.P., S.S., N.V., L.W., A.W., and F.I.W. performed research; A.D.F., T.T.R., and R. Keribin analyzed data; and A.D.F. wrote the paper.

The authors declare no conflict of interest.

This article is a PNAS Direct Submission. K.F. is a guest editor invited by the Editorial Board.

[1]To whom correspondence should be addressed. E-mail: adf10@cam.ac.uk.

This article contains supporting information online at www.pnas.org/lookup/suppl/doi:10.1073/pnas.1222477110/-/DCSupplemental.

four of which were DGVMs, were used in the Coupled Climate–Carbon Cycle Model Intercomparison Project (3). Terrestrial *NPP* and soil respiration responses to climate and CO_2 dominated the uncertainty of future atmospheric CO_2 levels. Ref. 4 looked at the responses of five DGVMs, coupled to a fast climate analog model, finding dramatic divergence in future behavior, particularly of tropical vegetation responses to drought and boreal ecosystem responses to elevated temperature and changing soil moisture. Ref. 5 looked in more detail at the responses of three of these DGVMs in the Amazon region, and found that although all three models simulated reductions in vegetation carbon, they did this for different reasons. LPJ mainly responded to precipitation, HyLand to humidity, and TRIFFID to the direct effects of temperature on physiology.

The main conclusion from these and similar studies is the significant uncertainty due to alternative model formulations of the fundamental physiological processes determining responses of *NPP*. This is perhaps surprising given that physiological processes have been intensively studied for many years, and similar approaches are used in the different models. In fact, the basic approaches incorporated into the early DGVMs have hardly changed over time.

Here seven GVMs are used to investigate possible responses of global natural terrestrial vegetation to a major new set of future climate and atmospheric CO_2 projections generated as part of the fifth phase of the Coupled Model Intercomparison Project (CMIP5) (6), the primary climate modeling contribution to the latest Intergovernmental Panel on Climate Change assessment. This study goes beyond previous work in the range of climate models, scenarios, and GVMs that are considered, and analyzes the outputs using an approach that gives equal weighting to production and turnover processes. Of the seven models used in the current study, HYBRID4 (7), JeDi (8), JULES (9), and LPJmL (10) simulated full vegetation dynamics, whereas ORCHIDEE (11), SDGVM (12), and VISIT (13, 14) used prescribed vegetation distributions. We discuss the simulated changes in ecosystem state in terms of underlying model behaviors and assumptions, assess the level of agreement between the GVMs and GVM×GCM combinations, and identify where key uncertainties remain. The overall outcome is a summary of the current state of knowledge concerning the impacts on terrestrial vegetation of future policy decisions that aim to influence anthropogenic greenhouse gas emissions. We recognize that much of the land surface will continue to be transformed by land use, but do not consider this forcing to focus on identifying the main discrepancies between vegetation models. However, it is clear that complete assessment of the role of the future terrestrial surface in the global climate system requires a sophisticated consideration of both natural and managed lands, and so all GVMs aimed at future predictions need to incorporate parameterizations of anthropogenically altered landscapes.

Results

Vegetation Carbon. To facilitate comparison across simulations using all GCMs and RCPs, we express global vegetation change with respect to change in global mean land surface temperature (ΔMLT). It is important to recognize that ΔMLT is a proxy for changing magnitudes of temperature, precipitation, humidity, and CO_2, and that both climate and ecosystem inertia also play roles in the relationships between climate forcing and vegetation responses.

Baseline (i.e., mean 1971–1999) global C_{veg} varies between 461 Pg C and 998 Pg C, and increases with ΔMLT for all vegetation models under all 110 climate and CO_2 increase scenarios (Fig. 1) (see *Materials and Methods* and *SI Text* for details of simulations). Global C_{veg} increases more-or-less linearly in all models up to about +4 °C, but with different slopes. At higher temperatures four of the models saturate, whereas the remaining three continue increasing. Intermodel mean C_{veg} stops increasing at +4 °C, where the full range of the increase is 52–477 Pg C, depending on the GVM×GCM×RCP combination. The mean increase of 224 Pg C over all models is equivalant to $\approx$24 y of recent global fossil fuel CO_2 emissions. Within-GVM variation is due to the different GCM climates and CO_2 mixing ratios.

The spatial distribution of the mean response across all 110 realizations that fall into the 3.5 °C–4.5 °C change bin is shown in Fig. 2. Despite the large spread between simulations, consistent spatial patterns are evident. Most land supports increased vegetation carbon, with simulations agreeing on this increase in many locations. Increases are particularly high across much of northern North America, northwestern and southeastern South America, the colder regions of western Europe, most of northern Eurasia, southeastern Asia, and tropical Africa.

There are also regions where vegetation carbon declines, including parts of southern North America, much of central South America, the southern Mediterranean region, southwestern Africa, and southwestern Australia. Declines range to −59% of current C_{veg}. The realizations are less in agreement concerning these declines than they are for regions of increase, except in the northern Maghreb. The spatial extent of the areas experiencing decreased vegetation carbon increases monotonically with warming above +3 °C, as does the intermodel agreement on these reductions. At ΔMLT = +7 °C, very large areas of South America, the Mediterranean region, and Australia experience mean decreases in C_{veg} relative to current values. Moreover, model agreement at the 90% level extends to southwestern Africa and Australia at these higher temperature increases. In contrast, model agreement on increases at +7 °C becomes less widespread than at lower warming, with the Tibetan Plateau, the Ethiopian Highlands, northeastern Siberia, and southwestern Canada still consistently experiencing higher C_{veg}. In addition, we find that an extensive region of the southern Sahara/northern Sahel experiences very large relative increases in vegetation carbon, although there is

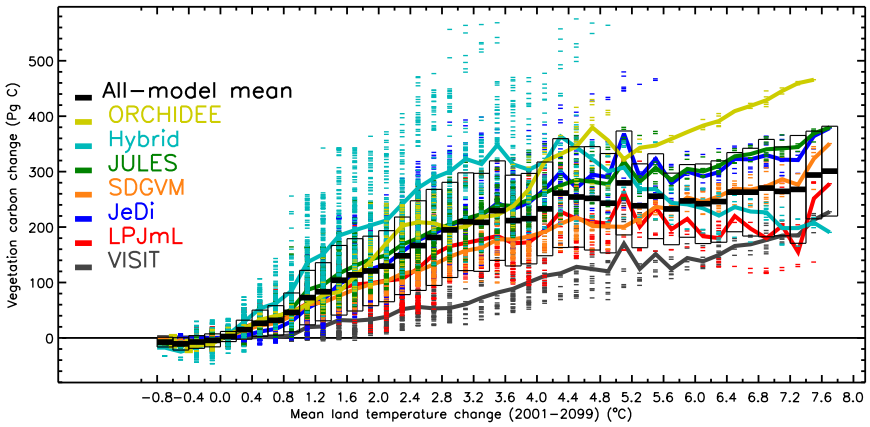

Fig. 1. Future global vegetation carbon change calculated by seven global vegetation models using climate outputs and associated increasing CO_2 from five GCMs run with four RCPs, expressed as the change from the 1971–1999 mean relative to change in global mean land temperature. The annual values for each model are shown for all simulations binned into 0.2-°C–wide bins (short, horizontal stripes; *n* for each bin varies from 6 to 857). The means for each model (thick colored lines) and the multimodel means and SDs (black bars and boxes) are also shown. Average CO_2 in the bins increases from 370 ppm at ΔMLT = 0 °C to 911 ppm at ΔMLT = 7.5 °C.

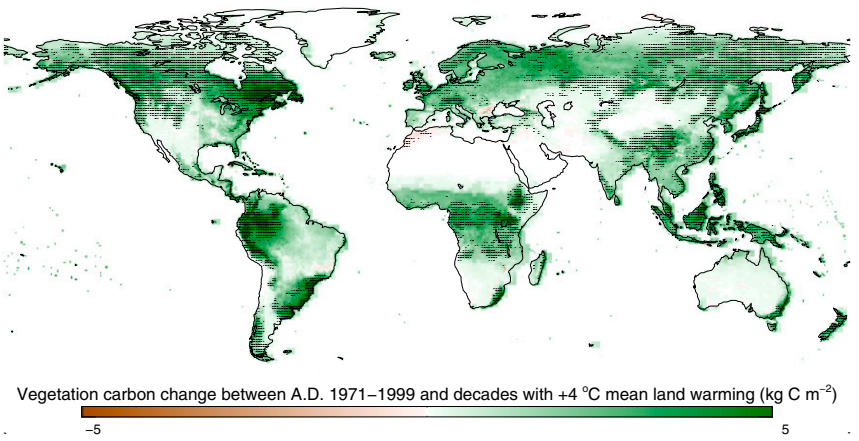

Fig. 2. Mean change in vegetation carbon at +4 °C global land warming from a 1971–1999 baseline. Values are changes averaged across all simulations and decades (i.e., GVM×GCM×RCP×decade, n = 110), binned into the mean-decadal 3.5 °C–4.5 °C change bin (CO_2 = 510–758 ppm; see Table S2 for details). Stippling shows where at least 90% of all realizations agree on the sign of change.

less agreement on this between simulations, primarily due to variation in climate predictions.

Variation between model simulations is greatest for C_{veg} change between current and +4 °C-binned simulations across the central United States, northeastern South America, southern Africa, the Near East, and much of Australia. These tend to be regions with increasing future moisture stress, which varies considerably between GCMs.

Model Differences. Focusing on the results from one of the GCM×RCP scenarios allows vegetation model behavior to be analyzed in more detail. The mean global land surface temperature in the Met Office Hadley Centre Global Environment Model version 2 - Earth System (HadGEM2-ES) RCP 8.5 simulation rises to ≈7.5 °C above current values, covering almost the entire spread of all GCM×RCP forcings. Furthermore, the global C_{veg} responses under this forcing (Fig. 3) are close to the mean responses of each vegetation model across all forcing scenarios. In other words, this GCM simulates average relationships between global mean warming and impact-relevant climate variables such as precipitation. Global C_{veg} increases remarkably linearly throughout the century in five vegetation models (i.e., ORCHIDEE, JeDi, JULES, SDGVM, and VISIT). In contrast, in LPJmL and HYBRID4 global C_{veg} saturates by about 2060, followed by a decline.

Changing C_{veg} results from changes in *NPP* and the residence time of carbon in living vegetation,

$$\frac{dC_{veg}}{dt} = NPP - \frac{C_{veg}}{\tau}, \qquad [1]$$

where τ is carbon residence time. This formulation is applied here both locally and globally as a difference equation over

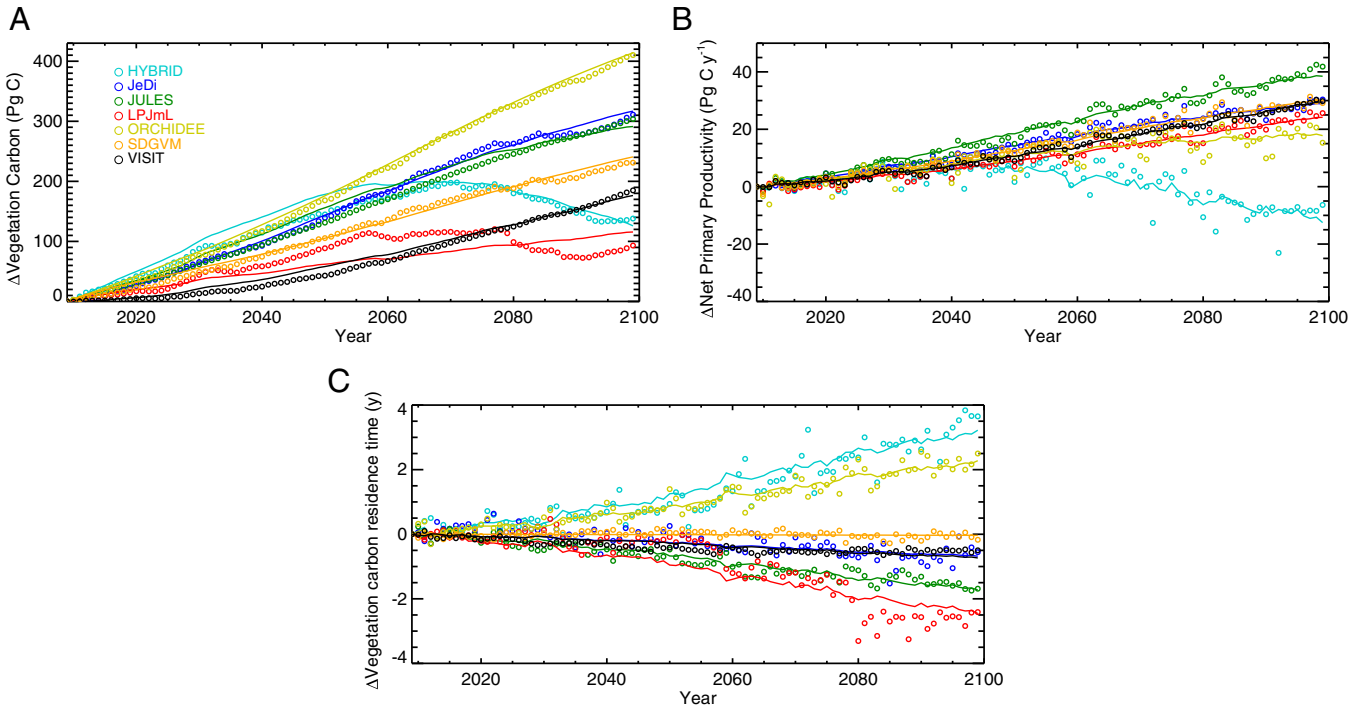

Fig. 3. (*A*–*C*) Change in annual global mean vegetation carbon (*A*), *NPP* (*B*), and residence time of carbon in vegetation (*C*) under the HadGEM2-ES RCP 8.5 climate and CO_2 scenario for seven global vegetation models. Symbols are GVM outputs and lines are fitted responses, using a simple model fitted to the global *NPP* responses to CO_2 and temperature and residence time responses to temperature for each model as described in the main text.

annual time steps, enabling annual residence time to be inferred from simulated *NPP* and ΔC_{veg}. In the vegetation models used here, *NPP* is responsive to climate and atmospheric CO_2, both directly and through indirect effects on vegetation development. Carbon residence time depends on the turnover rates of plant parts and the mortality rates of individuals, processes modeled using baseline rates, climate sensitivities (including fire), and competitively induced mortality, and are affected indirectly through shifts in vegetation composition, although not all these processes are treated in all models (*SI Text*).

All models except HYBRID4 display a linear increase in global *NPP* with time (Fig. 3). This is due to a saturating effect of CO_2 combined with a near-linear negative impact of climate change. In contrast, global mean annual residence time declines (JeDi, VISIT, JULES, and LPJmL), increases (HYBRID4 and ORCHIDEE), or does not change (SDGVM). Residence time in LPJmL remains fairly constant until about 2050 and then declines rapidly, whereas in VISIT it stabilizes in 2050 and in HYBRID4 it then increases more rapidly. These results suggest that the primary causes of the differences in the trajectories of future global C_{veg} between the GVMs are the different ways in which residence time responds to climate and CO_2, at least for the non-HYBRID4 models. Analyses of differences in model behavior should therefore focus not only on the processes of carbon acquisition (i.e., photosynthesis and *NPP*), but also on the dynamics of vegetation carbon turnover.

Using additional simulations with each GVM in which the CO_2 experienced by the vegetation was held constant, these results were further analyzed by fitting to each GVM globally, a simple two-parameter model for the relationship between *NPP* and CO_2 [i.e., $a_1\Delta C_a/(a_2+\Delta C_a)$, where ΔC_a is the change in CO_2], combined with linear models for the relationships between *NPP* and temperature (i.e., $a_3\Delta MLT$) and residence time and temperature (i.e., $a_4\Delta MLT$). The fitted global model is plotted as lines in Fig. 3 and is used to ascribe sources of uncertainty to different processes. The variance in final C_{veg} caused by differences in fitted residence time relationships between models was found to be 30% higher than that caused by differences in the fitted *NPP* responses when all models were considered. Leaving out HYBRID4, which displays a different *NPP* response, increases the effect of residence time to 151% more than that of *NPP*. In other words, for the non-HYBRID4 models, differences in residence time relationships with climate between the models are responsible for more than twice the variation in modeled global C_{veg} change to 2100 than are differences in *NPP* relationships with temperature and CO_2.

The HYBRID4 vegetation model includes a nitrogen cycle, and so this might be expected to be the reason for the decline in *NPP*, and hence C_{veg}, above 4 °C of warming because of the potential for nitrogen to limit CO_2 fertilization (e.g., ref. 15). However, further analysis showed that the decline in *NPP* is in fact due to increased vapor pressure deficits causing stomatal closure and increased evaporative demand over temperate and tropical forests, with increasing nitrogen mineralization reducing the potential constraint from N feedbacks (Fig. 4). There is considerable variability in the ways in which stomata respond to humidity between the models.

In contrast, the decline in C_{veg} after 2050 in LPJmL is driven by increases in turnover across the temperate and boreal forests (Fig. 4). Tree mortality increases as a consequence of increasing tissue mortality due to high-temperature periods and in response to water stress in these regions, with subsequent increasing transient dominance by C_3 grasses during slow regrowth of better-adapted tree types.

Declining residence times in JeDi, LPJmL, JULES, and VISIT with warming, as shown in Fig. 4, would by themselves lead to reduced C_{veg}, but these changes are more than compensated for by increases in *NPP* at the global scale (Fig. 3). Declining residence times in these models are due to temperature dependencies of turnover rates (processes included in the models and important for production and residence time differences are indicated symbolically in Fig. 4). In contrast, global mean residence time in HYBRID4 and ORCHIDEE increases. In HYBRID4 this is due to reduced tree mortality across the boreal forest as higher CO_2 concentrations and temperatures improve their carbon balance. Residence time of temperate and Amazon forest carbon in HYBRID4 is reduced with warming due to heat-induced increases in vapor pressure deficits leading to unfavorable carbon balances, which increase rates of individual mortality (Fig. 4). In ORCHIDEE residence time increases across much of the boreal forest and many tropical regions. These changes are due to a greater biomass of younger leaves, which increases with *NPP* and has lower intrinsic rates of turnover than those of older leaves.

In JeDi, residence time falls over much of the northern boreal and arctic region, as well as the tropics, whereas it increases across temperate latitudes (Fig. 4). In contrast, in JULES residence time decreases in midlatitude deciduous forests, but changes little elsewhere. These changes are driven by changing vegetation type mixtures, with grasses and smaller shrubs in JeDi decreasing boreal residence times, and greater proportions of trees increasing residence times in the southeastern United States and China. Large reductions in residence time in northeastern Amazonia in SDGVM, and more generally across the tropics in VISIT, occur in response to increased fire frequency.

Discussion

Using simulation results from five GCMs and the full range of RCPs, we have characterized the range of terrestrial vegetation responses to future conditions across seven different global vegetation model formulations. However, multiple sources of uncertainty in the chain from climate forcing to impact model limit confidence in specific predictions. Agreement nevertheless emerges on increases in future global vegetation carbon, with large regional increases across much of the boreal forest, western Amazonia, central Africa, western China, and southeastern Asia. Simulations also agree on decreases in parts of northern Africa. Furthermore, there is agreement on a general increase in the areal extent of regions with negative impacts above +3 °C of warming. The relative dominance of different plant types is also predicted to change, but there is little consensus among the models as to the details.

Previous modeling studies have also consistently predicted increased global vegetation carbon under future scenarios of climate and CO_2, but with considerable variation in absolute values (2–4). A relatively large additional land carbon pool has been viewed as implausible due to N constraints on additional plant growth (15, 16). However, N constraints in this study are not responsible for different responses to forcings. Nevertheless, better understanding of nutrient constraints in general, and of how to incorporate them into global vegetation models, is a major priority. Observational evidence strongly suggests that global vegetation carbon in natural forests is already increasing (17), and the relationship of any future increases with ΔMLT has important consequences for future levels of atmospheric CO_2. The results presented here contribute to our understanding of the likely range under different amounts of global mean warming.

Analyzing the responses of the GVMs in terms of the responses of carbon inputs (i.e., *NPP*) and outputs (i.e., 1/residence time) to climate and CO_2 helps to identify sources of model differences. Changes in *NPP* are more consistent between models than changes in residence time, which increases, decreases, or does not change over this century. LPJmL and HYBRID4 treat competitive interactions explicitly, either through competition between plant types (LPJmL), or between actual individuals using a gap model approach (HYBRID4), with increased mortality resulting from competition. However, residence time in these two models changes in opposite directions with respect to climate change. In contrast, it was found that when CO_2 was fixed, residence time declined with warming in both HYBRID4 and LPJmL, albeit with a significantly greater reduction in the latter model. The switch in the sign of response in HYBRID4 is due to the

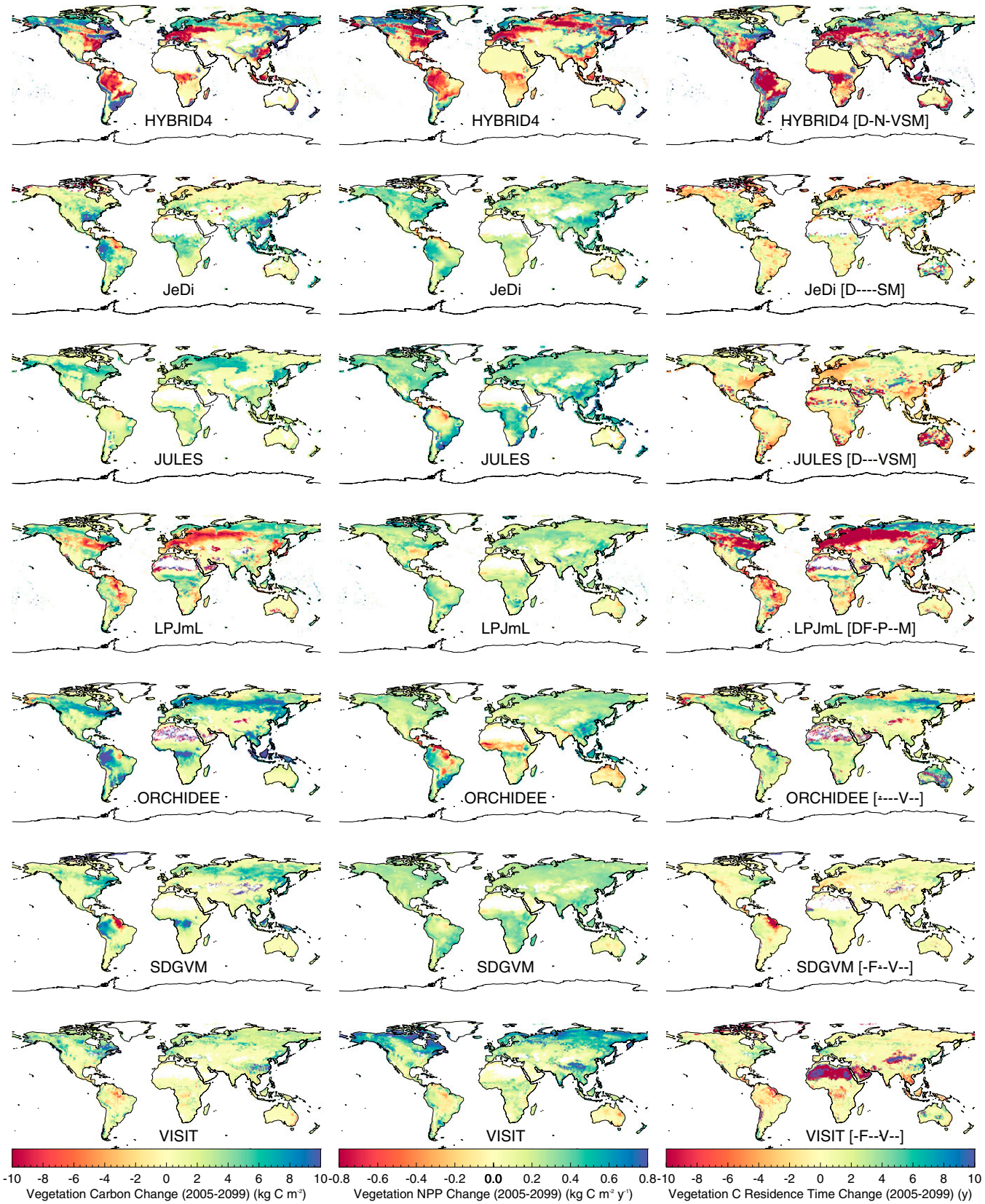

Fig. 4. Change in mean-decadal vegetation carbon, annual *NPP*, and vegetation carbon residence time simulated by seven GVMs under HadGEM2-ES RCP 8.5 forcings between A.D. 2005 and 2099. (*Right*) Letters indicate relevant processes for residence time and *NPP* behavior included in each model: D, dynamic vegetation; F, fire; N, N cycle; P, permafrost; V, vapor pressure deficit affects stomatal conductance; S, temperature affects senescence; and M, temperature affects mortality.

removal of the beneficial effects of increasing CO_2 on tree survival, leading to increased tree mortality with atmospheric evaporative demand. In JULES, on the other hand, residence time declines with warming when CO_2 also increases, yet increases with warming when CO_2 is fixed. This increase was responsible for JULES having almost no overall change in global C_{veg} when CO_2 was fixed, despite falling *NPP*. In ORCHIDEE, residence time also increased with warming when CO_2 was fixed, with little overall change in C_{veg}. It is clear from these results that the response of residence time to climate and CO_2 is a critical yet inconsistently represented feature of current global vegetation models.

Although it has been recognized for some time that differences in modeled *NPP* responses to climate and CO_2 are major sources of uncertainty in GVMs, there has been little discussion on the importance of residence time. A significant component of this key ecosystem characteristic is dependent on relatively slow processes such as rates of recuitment, mortality, and changes in vegetation composition. In contrast, validation exercises have focused on short-term carbon fluxes and leaf area dynamics, features readily observable (e.g., ref. 18). However, there is increasing recognition of the importance of demographic processes not just for compositional dynamics, but also for changes in carbon balance (e.g., ref. 19).

Discontinuities in vegetation responses at around 4 °C of global land surface warming across a number of the vegetation models indicate thresholds above which the positive impacts of increasing CO_2 become dominated by negative impacts of moisture stress at the global scale. In two models the threshold is expressed in *NPP*, in two it is in residence time, and in one it is in both. Further work should focus on confronting the processes and emergent model behavior responsible for these discontinuities with observational data. Spatial and temporal variability in carbon residence time and tree mortality is an obvious place to start, and although recent studies have identified important sources of relevant data (e.g., refs. 20 and 21), data on key processes such as mortality at large scales are rare. An exception is the authors of ref. 22, who interrogated a large eastern US forest inventory database for mortality dynamics. They found substantial spatial variation in mortality rates, driven by species-specific relationships with environmental factors. Future changes in mortality rates cannot therefore be predicted simply from current mortality/climate relationships. These data need to be fully understood at a mechanistic level, and used to inform methodologies for incorporating variation in mortality/environmental relationships into DGVMs.

Vegetation carbon residence time not only is important because of its contribution to GVM uncertainty, but also represents a key stage in the cascade of carbon from the atmosphere, through various organic and inorganic surface pools, and back to the atmosphere. Changes in vegetation carbon residence times can cause major shifts in the distribution of carbon between pools, overall fluxes, and the time constants of terrestrial carbon transitions, with consequences for the land carbon balance and the associated state of ecosystems. The model results presented here clearly demonstrate the need for increased understanding of the multifaceted dynamics of this key ecosystem property.

Materials and Methods

Daily climate forcings for the land area were provided for all four RCPs submitted as part of the fifth phase of the CMIP5 (6) from the following five GCMs: GFDL-ESM2M, HadGEM2-ES, IPSL-CM5A-LR, MIROC-ESM-CHEM, and NorESM1-M. The raw daily climate model simulation results were bias corrected according to the ISI-MIP protocol (1, 23), despite known caveats with respect to the use of bias correction in climate impact studies (24). The above results are based on simulations using these daily climate forcings from seven GVMs. These models are described in *SI Text*, including an overview of the main features responsible for the principal differences in behavior identified here (Table S1). In total, 110 simulations have been included in this analysis, as detailed in Table S3.

ACKNOWLEDGMENTS. The research leading to these results has received funding from the European Community's Seventh Framework Programme (FP7 2007-2013) under Grant 238366. R.B., R.K., R.D., A.W., and P.D.F. were supported by the Joint Department of Energy and Climate Change/Department for Environment, Food and Rural Affairs Met Office Hadley Centre Climate Programme (GA01101). A.I. and K.N. were supported by the Environment Research and Technology Development Fund (S-10) of the Ministry of the Environment, Japan. We acknowledge the World Climate Research Programme's Working Group on Coupled Modelling, which is responsible for the Coupled Model Intercomparison Project (CMIP), and we thank the climate modeling groups responsible for the GFDL-ESM2M, HadGEM2-ES, IPSL-CM5A-LR, MIROC-ESM-CHEM, and NorESM1-M models for producing and making available their model output. For CMIP, the US Department of Energy's Program for Climate Model Diagnosis and Intercomparison provides coordinating support and led development of software infrastructure in partnership with the Global Organization for Earth System Science Portals. This work has been conducted under the framework of the Inter-Sectoral Impact Model Intercomparison Project (ISI-MIP). The ISI-MIP Fast Track project was funded by the German Federal Ministry of Education and Research (BMBF) with project funding Reference 01LS1201A.

1. Warszawski L, et al. (2014) The Inter-Sectoral Impact Model Intercomparison Project (ISI–MIP): Project framework. *Proc Natl Acad Sci USA* 111:3228–3232.
2. Cramer W, et al. (2001) Global response of terrestrial ecosystem structure and function to CO_2 and climate change: results from six dynamic global vegetation models. *Glob Change Biol* 7:357–373.
3. Friendlingstein, et al. (2006) Climate-Carbon Cycle Feedback analysis: Results from the C^4MIP Model Intercomparison. *J Clim* 19:3337–3353.
4. Sitch S, et al. (2008) Evaluation of the terrestrial carbon cycle, future plant geography and climate-carbon cycle feedbacks using five Dynamic Global Vegetation Models (DGVMs). *Glob Change Biol* 14:2015–2039.
5. Galbraith D, et al. (2010) Multiple mechanisms of Amazonian forest biomass losses in three dynamic global vegetation models under climate change. *New Phytol* 187(3): 647–665.
6. Taylor KE, Stouffer RJ, Meehl GA (2012) An overview of CMIP5 and the experiment design. *Bull Am Meteorol Soc* 93:485–498.
7. Friend AD, White A (2000) Evaluation and analysis of a dynamic terrestrial ecosystem model under preindustrial conditions at the global scale. *Global Biogeochem Cycles* 14:1173–1190.
8. Pavlick R, Drewry DT, Bohn K, Reu B, Kleidon A (2012) The Jena Diversity-Dynamic Global Vegetation Model (JeDi-DGVM): a diverse approach to representing terrestrial biogeography and biogeochemistry based on plant functional trade-offs. *Biogeosciences* 10:4137–4177.
9. Clark DB, et al. (2011) The Joint UK land environment simulator (JULES), model description - Part 2: Carbon fluxes and vegetation dynamics. *Geoscientific Model Development* 4:701–722.
10. Sitch S, et al. (2003) Evaluation of ecosystem dynamics, plant geography and terrestrial carbon cycling in the LPJ dynamic global vegetation model. *Glob Change Biol* 9(2):161–185.
11. Krinner G, et al. (2005) A dynamic global vegetation model for studies of the coupled atmosphere-biosphere system. *Global Biogeochem Cycles* 19:GB1015.
12. Woodward FI, Lomas MR (2004) Vegetation dynamics - simulating responses to climatic change. *Biol Rev Camb Philos Soc* 79(3):643–670.
13. Ito A, Oikawa T (2002) A simulation model of the carbon cycle in land ecosystems (Sim-CYCLE): a description based on dry-matter production theory and plot-scale validation. *Ecol Modell* 151(2-3):143–176.
14. Inatomi M, Ito A, Ishijima K, Murayama S (2010) Greenhouse gas budget of a cool-temperate deciduous broad-leaved forest in Japan estimated using a process-based model. *Ecosystems* 13:472–483.
15. Luo Y, et al. (2004) Progressive nitrogen limitation of ecosystem responses to rising atmospheric carbon dioxide. *Bioscience* 54:731–739.
16. Hungate BA, Dukes JS, Shaw MR, Luo Y, Field CB (2003) Nitrogen and climate change. *Science* 302(5650):1512–1513.
17. Pan Y, et al. (2011) A large and persistent carbon sink in the world's forests. *Science* 333(6045):988–993.
18. Randerson JT, et al. (2009) Systematic assessment of terrestrial biogeochemistry in coupled climate-carbon models. *Glob Change Biol* 15:2462–2484.
19. Purves D, Pacala S (2008) Predictive models of forest dynamics. *Science* 320(5882): 1452–1453.
20. Allen CD, et al. (2010) A global overview of drought and heat-induced tree mortality reveals emerging climate change risks for forest. *For Ecol Manage* 259:660–684.
21. Galbraith D, et al. (2013) Residence times of woody biomass in tropical forests. *Plant Ecol Divers* 6(1):139–157.
22. Lines ER, Coomes DA, Purves DW (2010) Influences of forest structure, climate and species composition on tree mortality across the eastern US. *PLoS ONE* 5(10):e13212, 10.1371/journal.pone.0013212.
23. Hempel S, Frieler K, Warszawski L, Schewe J, Piontek F (2013) A trend-preserving bias correction - the ISI-MIP approach. *Earth System Dynamics* 4:219–236.
24. Ehret U, Zehe E, Wulfmeyer V, Warrach-Sagi K, Liebert J (2012) Should we apply bias correction to global and regional climate model data? *Hydrol Earth Syst Sci* 16: 3391–3404.

Supporting Information

Friend et al. 10.1073/pnas.1222477110

SI Text

Global Vegetation Models Used in This Study

Seven global vegetation models (GVMs) were used in this study: HYBRID4 (1), JeDi (2), JULES (3), LPJmL (4, 5), ORCHIDEE (6, 7), SDGVM (8), and VISIT (9, 10). The vegetation models were used to simulate the responses of natural terrestrial vegetation to climate and CO_2 mixing ratio changes at 0.5°x0.5° (except for JULES and JeDi, which were run at 1.25°x1.85°) spatial resolution over 1951–2099.

The total time duration of the spin-up varied among the vegetation models in order to accommodate differences in reaching equilibrium for multiple state variables. As spin-up climatology, the detrended and bias-corrected daily climate inputs for three consecutive decades spanning 1951–1980 were provided for each GCM (JULES used HadGEM2-ES climate for all spin-ups). Except for JULES, if the spin-up required more than 30 y, every second 30-y period was inverted (i.e., 1980–1951), to avoid artifacts due to discontinuities in the climate data. The CO_2 mixing ratio during the spin-up and historical periods was fixed at 280 ppm for all years before 1765, and was thereafter increased linearly until 2005 (2004 for HadGEM2-ES and 2000 for fixed CO_2 runs). CO_2 mixing ratio was then changed according to the RCP until 2099 (or fixed at the 2001 value for the no CO_2 change runs).

Key GVM features relevant to the results presented in this paper are given in Table S1, and overall model descriptions are given below.

HYBRID4

HYBRID4 simulates the growth and competitive interactions of individual trees using a gap-model approach, with an herbaceous understory. Individual trees can belong to one of six generalized plant types, and the understory can be of either C_3, C_4, or mixed leaf physiology. Twenty independent plots were simulated for each terrestrial gridbox using a daily timestep. A relatively simple surface physics and hydrology routine calculates the daytime and nighttime surface temperatures and soil moisture dynamics over two soil water layers. Trees have access to both layers whereas the herbaceous layer only accesses the upper layer. A nitrogen cycle is included, which affects canopy photosynthetic capacities. Atmospheric N deposition was assumed to be spatially and temporally invariant. Individual tree mortality can occur as a result of low labile carbon, and is influenced by overall rates of photosynthesis and respiration. Photosynthesis is calculated using a standard Farquhar-type model. Stomatal conductance is calculated using empirical functions of vapor pressure deficit (VPD), temperature, CO_2, shortwave radiation, soil moisture, and photosynthetic capacity. Both photosynthesis and respiration are scaled to the canopy using a "big-leaf" approach. Maintenance respiration is a function of tissue N contents and temperature. Detailed canopy radiation transfer is calculated across foliage layers. All plant types are assumed to be available for growth in all plots, but only those that are competitively successful will survive and grow. For full details concerning HYBRID4 please refer to ref. 1.

JeDi

JeDi simulates the performance of a large number of randomly-generated plant growth strategies (~2000), constrained by ecophysiological trade-offs, within a coupled land surface hydrology module. All plant types are assumed to be available at all locations, but only those that are adequately adapted to the local conditions will survive and grow. Gridbox properties are scaled using the biomass-ratio hypothesis. This diverse representation of vegetation provides more flexibility for ecosystem composition to adapt to environmental changes. Growth and surface processes are simulated on a daily timestep. The growing period depends on soil moisture availability and surface temperature. Baseline turnover rates are fixed for each growth strategy, but there is also a senescence component which depends on overall net primary productivity (NPP). Photosynthesis is a function of absorbed shortwave radiation and photosynthetic capacity, determined by temperature, atmospheric CO_2, and canopy N. Transpiration and photosynthesis are both down-regulated by a moisture-stress factor which accounts for both soil water supply and atmospheric demand (defined using the Priestley-Taylor equation). Maintenance respiration is a function of tissue N content and temperature. The depth of the single soil moisture layer representing the rooting zone of each growth strategy is determined by plant coarse root biomass. For full details concerning JeDi please refer to ref. 2.

JULES

JULES represents the dynamics of five plant types within each gridbox using a Lotka-Volterra approach. Surface physics are simulated using a sophisticated GCM land surface scheme with a 30 to 60 min timestep. Photosynthesis of each plant type is calculated using a standard Farquhar-type approach, with a moisture stress factor applied directly to leaf photosynthesis. Stomatal conductance is calculated using an empirical function of net photosynthesis, CO_2, and VPD. Scaling to the canopy uses a big-leaf approximation with a two-stream approximation of canopy radiation interception. Maintenance respiration rates depend on tissue N contents and temperatures. For full details concerning JULES please refer to ref. 3.

LPJmL

LPJmL simulates the dynamics of nine plant types on a daily timestep, each with different physiological tolerances. The relative contribution of plant types to overall gridbox properties is based on its relative fractional coverage. This cover is proportional to the leaf area index and crown area of an average individual of each woody plant type in the gridbox, together with its population density, and the herbaceous understory. Each plant type also has bioclimatic limits that determine whether it can survive and/or regenerate under a particular climatic regime. The permafrost model includes an energy balance model, including one-dimensional heat conduction, convection of latent heat, freezing, and thawing mechanics. Soil hydrology is calculated using 5 layers with different rooting distributions for different plant types. The Farquhar-based photosynthesis is calculated from absorbed radiation, temperature, CO_2, and soil moisture status. Maintenance respiration is proportional to tissue N contents and temperature. Plant tissues turn over at fixed rates but there is also a calculation of annual mortality of individuals. Competition-driven mortality occurs if the total space available is insufficient for the sum of the fractional covers. Mortality also occurs in proportion to growth efficiency (i.e., the ratio of biomass increment to leaf area) and in response to heat stress. A fire module is included, which depends on fuel load and litter moisture. Establishment of new plant is filtered depending in bioclimatic limits. LPJmL's agricultural modules simulating fractions of crop and bioenergy plants were deactivated for these runs. For full details concerning LPJmL please refer to refs. 4 and 5.

ORCHIDEE

ORCHIDEE was applied in this project using a prescribed plant functional type distribution corresponding to pre-industrial land cover, which was kept constant for the duration of the simulations. The model therefore simulated no change in vegetation distribution. Twelve plant types are represented, and photosynthesis is simulated using a standard Farquhar-model approach coupled to the Ball-Berry stomatal conductance model. Photosynthetic capacity is directly affected by soil moisture stress (a scaling factor that decreases linearly to zero when root extractable water drops below a threshold of 0.4), and leaf age, as well as plant type, and indirectly through the atmospheric stress impacting the Ball-Berry conductance. Scaling of photosynthesis and stomatal conductance to the canopy level is achieved using a big-leaf approximation. Maintenance respiration is a function of tissue biomass and temperature. Turnover occurs due to phenological responses of leaves and fine roots, herbivory (fixed rates), and leaf aging. Mortality is prescribed as a fixed ratio of standing biomss. For full details concerning ORCHIDEE please refer to ref. 6. The ORCHIDEE AR5 version used in this study contains an improved description of phenology (7).

SDGVM

Like ORCHIDEE, SDGVM also used a fixed vegetation distribution for this study. Seven plant types are simulated, with photosynthesis proportional to leaf area and internal leaf CO_2. The latter is calculated as a function of N uptake rate, shortwave radiation, temperature, and VPD. Soil moisture affects leaf area. Maintenance respiration is a function of N uptake and tissue temperature. A surface physics routine calculates temperatures and soil moisture dynamics. Fire is simulated as a function of moisture stress and vegetation state. For full details concerning SDVGM please refer to ref. 8.

VISIT

VISIT was also run with a fixed prescribed vegetation distribution. The Olson vegetation data map was used for biome type reference. The carbon dynamics of 16 plant types are simulated, with photosynthesis an empirical function of the incident shortwave radiation, canopy leaf area index, attenuation coefficient, leaf-level light-use efficiency, and maximum photosynthetic rate. The light-use efficiency and maximum photosynthetic rate are functions of temperature, intercellular CO_2 concentration, and soil water content, taking into account biome-specific ecophysiological characteristics. The growth respiration rate is proportional to the amount of carbon allocated to each organ, whereas the maintenance respiration rate increases linearly with standing biomass and exponentially with temperature. Growth and maintenance respirations are separately estimated for leaves, stems, and roots. Stomatal conductance is calculated using the Leuning version of the Ball-Berry model. A leaf area optimization routine is used to determine allocation of labile carbon to the canopy. Fixed rates of turnover are applied to all tissues. A simple soil hydrology routine simulates the dynamics of two soil water layers. For full details concerning VISIT please refer to refs. 9 and 10.

1. Friend AD, White A (2000) Evaluation and analysis of a dynamic terrestrial ecosystem model under preindustrial conditions at the global scale. *Global Biogeochemical Cycles* 14:1173–1190.
2. Pavlick R, Drewry DT, Bohn K, Reu B, Kleidon A (2012) The Jena Diversity-Dynamic Global Vegetation Model (JeDi-DGVM): a diverse approach to representing terrestrial biogeography and biogeochemistry based on plant functional trade-offs. *Biogeosciences* 10:4137–4177.
3. Clark DB, et al. (2011) The Joint UK land environment simulator (JULES), model description - Part 2: carbon fluxes and vegetation dynamics. *Geoscientific Model Development* 4:701–722.
4. Sitch S, et al. (2003) Evaluation of ecosystem dynamics, plant geography and terrestrial carbon cycling in the LPJ dynamic global vegetation model. *Global Change Biology* 9:161–185.
5. Schaphoff S, et al. (2013) Contribution of permafrost soils to the global carbon budget. *Environmental Research Letters* 8:014026.
6. Krinner G, et al. (2005) A dynamic global vegetation model for studies of the coupled atmosphere-biosphere system. *Global Biogeochemical Cycles* 19:GB1015.
7. Maignan F, et al. (2011) Evaluation of a Global Vegetation Model using time series of satellite vegetation indices. *Geoscientific Model Development* 4:1103–1114.
8. Woodward FI, Lomas MR (2004) Vegetation dynamics - simulating responses to climatic change. *Biological Reviews* 79:643–670.
9. Ito A, Oikawa T (2002) A simulation model of the carbon cycle in land ecosystems (Sim-CYCLE): a description based on dry-matter production theory and plot-scale validation. *Ecological Modelling* 151:143–176.
10. Inatomi M, Ito A, Ishijima K, Murayama S (2010) Greenhouse gas budget of a cool-temperate deciduous broad-leaved forest in Japan estimated using a process-based model. *Ecosystems* 13:472–483.

Table S1. Effects of atmospheric humidity and temperature on processes responsible for major differences in *NPP* and residence time responses among seven analyzed GVMs

	Atmospheric temperature on turnover			Atmospheric temperature on mortality components					Atmospheric vapor pressure deficit on stomatal closure	
GVM	roots	stems	leaves	background	competition	C balance	fire	other	incl.	description
HYBRID4	✓	✓	✓	o	✓	✓	x	embolism	✓	stomatal closure as a direct function of *inter alia* vapor pressure deficit
JeDi	o	o	o	o	x	✓	x	none	x	water stress factor on GPP instead determined by evaporative demand and supply
JULES	✓	✓	✓	✓	x	x	x	none	x	Ball-Berry model
LPJmL	o	o	o	✓	✓	✓	✓	heat stress	x	water stress factor on GPP instead determined by soil moisture only
ORCHIDEE	o	o	o	x	x	x	x	none	x	Ball-Berry model
SDGVM	o	o	o	o	x	x	✓	none	✓	stomatal closure as a function of relative humidity and temperature
VISIT	o	o	o	x	x	x	x	none	x	Ball-Berry model

A "✓" means that the formulation is dependent on the respective variable, while an "o" means that the process is incorporated but not dependent on the respective variable, and an "x" means the process is not explicitly treated.

Table S2. Number of decades of each GVMxGCMxRCP combination in each mean-decadal 1-degree wide land temperature change bin classified by GCM, RCP, and temperature bin

ΔT (°C) CO_2min (ppm) CO_2max (ppm)	RCP	GFDL-ESM2M	HadGEM2-ES	IPSL-CM5A-LR	MIROC-ESM-CHEM	NorESM1-M	Total
+1	2.6	60	14	12	12	20	118
370	4.5	16	12	15	10	12	65
510	6.0	30	14	15	15	16	90
	8.5	18	14	12	12	15	71
	Total	124	54	54	49	63	344
+2	2.6	0	56	48	42	30	176
391	4.5	24	12	10	15	16	77
594	6.0	10	21	10	10	12	63
	8.5	18	7	12	12	10	59
	Total	52	96	80	79	68	375
+3	2.6	0	0	0	6	0	6
426	4.5	0	12	25	15	12	64
594	6.0	10	14	15	10	12	61
	8.5	12	14	6	6	10	48
	Total	22	40	46	37	34	179
+4	2.6	0	0	0	0	0	0
510	4.5	0	24	0	10	0	34
758	6.0	0	14	10	10	0	34
	8.5	12	7	12	6	5	42
	Total	12	45	22	26	5	110
+5	2.6	0	0	0	0	0	0
610	4.5	0	0	0	0	0	0
926	6.0	0	7	0	5	0	12
	8.5	0	7	6	12	10	35
	Total	0	14	6	17	10	47
+6	2.6	0	0	0	0	0	0
684	4.5	0	0	0	0	0	0
844	6.0	0	0	0	0	0	0
	8.5	0	14	6	6	0	26
	Total	0	14	6	6	0	26
+7	2.6	0	0	0	0	0	0
853	4.5	0	0	0	0	0	0
926	6.0	0	0	0	0	0	0
	8.5	0	7	6	6	0	19
	Total	0	7	6	6	0	19

The CO_2 mixing ratio ranges are given for each bin. The range of CO_2 mixing ratios for each temperature bin reflects the different climate sensitivities of the five GCMs as well as the different trajectories of RCP forcings (i.e., warming continues after forcing is halted due to lagged responses in RCPs 2.6 and 4.5).

Table S3. Number of simulations for each GVMxGCMxRCP combination

GCM	RCP	HYBRID4	JeDi	JULES	LPJmL	ORCHIDEE	SDGVM	VISIT	Total
GFDL-ESM2M	2.6	1	1	1	1	0	1	1	6
	4.5	0	1	1	1	0	1	0	4
	6.0	1	1	1	1	0	1	0	5
	8.5	1	1	1	1	0	2	1	7 (6)
HadGEM2-ES	2.6	2	2	2	2	2	1	1	12 (7)
	4.5	2	2	2	2	0	1	1	10 (6)
	6.0	2	2	2	2	1	1	1	11 (7)
	8.5	2	2	2	2	2	2	2	14 (7)
IPSL-CM5A-LR	2.6	1	1	1	1	0	1	1	6
	4.5	1	1	1	1	0	1	0	5
	6.0	1	1	1	1	0	1	0	5
	8.5	1	1	1	1	0	2	1	7 (6)
MIROC-ESM-CHEM	2.6	1	1	1	1	0	1	1	6
	4.5	1	1	1	1	0	1	0	5
	6.0	1	1	1	1	0	1	0	5
	8.5	1	1	1	1	0	2	1	7 (6)
NorESM1-M	2.6	1	1	1	1	0	0	1	5
	4.5	1	1	1	1	0	0	0	4
	6.0	1	1	1	1	0	0	0	4
	8.5	1	1	1	1	0	0	1	5
	Total	23 (19)	24 (20)	24 (20)	24 (20)	5 (3)	20 (16)	13 (12)	133 (110)

When two runs are listed for a single combination, the additional run was with fixed CO_2 mixing ratio from 2001 onwards. The total number is given with (without) the number of runs with fixed CO_2 mixing ratio.